1 **A mechanosensitive channel Pkd2 modulates the assembly of myosin II and actin filaments**
2 **in the cytokinetic contractile ring**

3 Pritha Chowdhury, Debatrayee Sinha, Abhishek Poddar, Madhurya Chetluru and Qian Chen*
4 Department of Biological Sciences
5 The University of Toledo
6 2801 Bancroft St, Toledo, OH 43606
7 * Correspondence: qian.chen3@utoledo.edu

8

9 **Keywords:** Cytokinesis, Fission yeast, Myosin, Actin, Polycystin, Pkd2

10

11 **Running title:** Pkd2 regulates contractile ring assembly

Abstract

Cytokinesis, the last step in cell division, leads to the separation of daughter cells. This evolutionarily conserved process requires the force generated by an actomyosin contractile ring assembled at the equatorial plane. A newly discovered ion channel Pkd2 localizes to the equatorial plane and its activation by membrane-stretching promotes the cytokinetic calcium spikes in the fission yeast *Schizosacchromyces pombe* cells. Here, we investigated whether Pkd2 plays a direct role in the assembly and constriction of the contractile ring through quantitative fluorescence microscopy and genetic analyses. The localization of type II myosin Myo2, its regulatory light chain Rlc1 and actin filaments all increased in the contractile ring of a hypomorphic mutant *pkd2-81KD*, compared to the wild type. This was accompanied by a significant increase of the intracellular concentration of Rlc1 and actin filaments. A strong negative interaction existed between *pkd2-81KD* and the temperature-sensitive mutant *myo2-E1*. The *pkd2 myo2* double mutant cells failed to assemble a complete contractile ring and separate efficiently, even at the permissive temperature. We conclude that Pkd2 modulates the assembly of myosin and actin in the contractile ring, suggesting that this ion channel mediates a novel pathway to regulate the actin cytoskeletal dynamics during cytokinesis. (197 words)

Introduction

Cytokinesis is the last stage of cell division when the daughter cells separate physically through mechanical force. In most eukaryotes, this process requires an actomyosin contractile ring specifically assembled at the equatorial division plane. Decades of work have discovered several key signaling pathways that regulate the assembly and constriction of the contractile ring (for a review see (Pollard and Wu, 2010)). They include those mediated by Polo kinase, the Central Spindlin complex, and RhoA. These pathways in turn reorganize the actin cytoskeletal structures

35 to assemble the cytokinetic contractile ring which consists of dozens actin-binding proteins
36 including formin, cofilin and myosins (Balasubramanian et al., 1998; Chen and Pollard, 2011;
37 Kovar et al., 2011; Wu and Pollard, 2005). Among them, type II non-muscle myosins (Myosin
38 II) play a critical role by driving both the assembly of actin filaments in the contractile ring and
39 the ensuing ring constriction and disassembly of actin filaments from the ring (Balasubramanian
40 et al., 1998; Laplante et al., 2015; Malla et al., 2022). Myosin II is a motor protein whose
41 activities depend on its regulatory light chain (Rlc). However, it remains unknown how myosin
42 II toggles switch its initial function of assembling the contractile ring to the later role of
43 disassembly as cytokinesis progresses.

44 We recently made a surprising finding that an essential ion channel Pkd2 is required for
45 cytokinesis of the model organism fission yeast *Schizosacchromyces pombe* (Morris et al., 2019;
46 Palmer et al., 2005). As a transmembrane protein, Pkd2 is trafficked to the plasma membrane
47 where its distribution is cell-cycle dependent (Malla et al., 2023). During interphase, this channel
48 mostly localizes at the cell tips. Upon entering cytokinesis, Pkd2 is recruited to the cleavage
49 furrow where it stays until the end of cell separation. Pkd2 is an essential gene. A hypomorphic
50 mutant *pkd2-81KD*, which replaces the endogenous promoter with an inducible 81nmt1
51 promoter, reduces the expression of *pkd2* gene by more than 70%. Although this mutation
52 accelerates the cleavage furrow, the mutant cells often fail to separate at the end of cytokinesis
53 (Morris et al., 2019).

54 Pkd2 is a putative Ca^{2+}-permissive channel, activated by the membrane stretching. In
55 vitro reconstituted Pkd2 in giant unilamellar vesicles (GUV) allows the passage of Ca^{2+} when the
56 membrane is stretched by hydraulic force (Poddar et al., 2022). In vivo, Pkd2 promotes the
57 separation calcium spikes, the transient influx of Ca^{2+} following the daughter cell separation at

58 the end of cytokinesis (Poddar et al., 2021). Besides cytokinesis, Pkd2 also promotes the tip
59 extension of fission yeast cells during interphase (Sinha et al., 2022). To our knowledge, Pkd2 is
60 the only essential mechanosensitive ion channels identified so far in yeast.

61 Evolutionally, Pkd2 belongs to a conserved family of cation channels. Compared to
62 fission yeast, most vertebrates possess two polycystins, PC-1 and PC-2, encoded by Pkd1 and
63 Pkd2 genes respectively (for a review, see (Hu and Harris, 2020)). Both are essential but they
64 play distinct developmental roles (for reviews, see (Hardy and Tsiokas, 2020; Ta et al., 2020)).
65 PC-1 is a G-protein Coupled Receptor (GPCR) like protein. It possesses a large extracellular
66 domain (>100 KD) and a 11-helix transmembrane domain. In comparison, PC-2 is a classical
67 Transient Receptor Potential (TRP) channel with six transmembrane helices. Although PC2 can
68 oligomerizes by itself into a tetrameric cation channel (Shen et al., 2016), PC-1 and PC-2 are
69 also capable of assembling into a heterologous tetrameric channel in 3:1 ratio (Su et al., 2018).
70 Mutations of human polycystins lead to a common genetic disorder, Autosomal Dominant
71 Polycystic Kidney Disorder (ADPKD) (1994; Mochizuki et al., 1996). However, the cellular
72 function of polycystins, particularly in the context of cell division (AbouAlaiwi et al., 2011), has
73 remained largely unknown.

74 In this study, we focused on answering one question, does Pkd2 have a role in the
75 assembly of contractile ring during cytokinesis. Using quantitative fluorescence microscopy, we
76 measured the number of type II myosin Myo2, myosin regulatory light chain Rlc1 and actin in
77 the contractile ring of a hypomorphic mutant *pkd2-81KD* (Morris et al., 2019), in comparison to
78 the wild-type. Surprisingly, the number of all three proteins increased in the contractile ring of
79 the *pkd2* mutant cells. Genetic analysis revealed a negative interaction between two *pkd2*
80 mutants and the temperature-sensitive *myo2-E1* mutant. The *pkd2-B42 myo2-E1* mutant cells

81 grew very slowly even at the permissive temperature. These *pkd2 myo2* mutant cells assembled
82 their contractile ring very slowly. They failed to septate and lysed frequently. Overall, our results
83 would demonstrate that Pkd2 does modulate the assembly of myosin II and actin in the
84 contractile ring, suggesting the existence of a novel calcium signaling pathway mediated by this
85 mechanosensitive channel for reorganizing the actin cytoskeletal structures during cell division.

86 **Materials and methods**

87 **Cell culture and Yeast genetics**

88 Yeast cell culture and genetics were carried out according to the standard protocols (Moreno et
89 al., 1991). Unless specified, YE5S was used in all experiments. For genetic crosses, tetrads were
90 dissected using Sporeplay+ dissection microscope (Singer, England). Yeast strains used in this
91 study are listed in Table 1.

92 For ten-fold dilution series of yeast, overnight cultures were diluted and inoculated for
93 additional 5 hours before being spotting onto YE5s agar plates. The plates were incubated for 2-3
94 days before being scanned using a photo scanner (Epson).

95 **Microscopy**

96 For live microscopy, fission yeast cells were first inoculated in YE5s liquid media for two days
97 before being harvested through centrifugation at 1500g for 1 min during exponential phase at a
98 density between $5x10^6$ /ml and $1.0x10^7$/ml. The cells were resuspended in 50µl of YE5s and 6 µl
99 of the resuspended cells were spotted onto a gelatin pad (25% gelatin in YE5s) on a glass slide.
100 The cells were sealed under a coverslip (#1.5) with VALAP (1:1:1 mixture of Vaseline, lanolin
101 and paraffin) before imaging.

102 Confocal microscopy was carried out on a spinning disk confocal microscope equipped
103 with an EM-CCD camera. The Olympus IX71 microscope was equipped with three objective

104 lenses of 40x (NA=1.30, oil), 60x (NA=1.40, oil) and 100x (NA=1.40, oil), a motorized Piezo Z
105 Top plane (ASI, USA) and a confocal spinning disk unit (CSU-X1, Yokogawa, Japan). The
106 images were captured on an Ixon-897 EMCCD camera (Andor). Solid state lasers of 488 and
107 561nm were used to excite green and red fluorescence proteins respectively. Unless specified,
108 the cells were imaged with Z-series of 15 slices at a step size of 0.5um.

109 To stain the cell wall with calcofluor, exponentially growing cell culture was fixed with
110 4% paraformaldehyde, prepared from 16% fresh stock solution (Electron Microscopy Science,
111 USA). The fixed cells were washed with TEMK buffer (50mM Tris-HCL pH 7.4, 1mM $MgCl_2$,
112 50mM KCl,1mm EGTA, pH8.0) and stored in 1ml of TEMK overnight at 4ºC. The cells were
113 stained with 1µg/ml calcofluor, prepared with the stock solution (1mg/ml, Sigma Aldrich) on a
114 rocker for 10 minutes at the room temperature in the dark. The stained cells were pelleted and
115 resuspended in 50ul TEMK, 6ul of which was spotted on a glass slide directly and sealed under a
116 coverslip (#1.5) with VALAP. The images were acquired in an Olympus IX81 microscope
117 equipped with 60x objective lens (NA=1.42), a LED lamp for bright-field microscopy, and a
118 mercury lamp for fluorescence microscope. The images were captured on an ORCA C-11440
119 digital camera (Hamamatsu, Japan), operated with CellSens (Olympus).

120 **Image analysis**

121 We used ImageJ (NIH), its plug-ins and macros to process all the microscopy images. For
122 quantitative analysis, the time-lapse series were first corrected for X-Y drifting using the plugin
123 StackReg (Thevenaz et al., 1998). Average intensity projections of Z-series were used for
124 quantification. The localization of GFP-Myo2 and Rlc1-tdTomato at the contractile ring was
125 quantified by measuring the fluorescence intensities in a 1µm by 4µm rectangle centered on the
126 equatorial division plane. The measurements were corrected for the background fluorescence,

127 measured in a 0.2µm by 4µm rectangle adjoined to the equatorial division plane. To measure
128 fluorescence intensities of GFP-Lifeact in the contractile ring, we used the fluorescence of Rlc1-
129 tdTomato to manually segment the contractile ring. To determine the start of the contractile ring
130 constriction, we constructed kymographs based on the time-lapse series of the contractile ring.
131 All figures were prepared with Canvas X (ACD Systems) and the plots were prepared
132 using Origin 2021 (OriginLab, USA).

133 **Results**

134 **Pkd2 modulates the assembly of Myo2, Rlc1, and actin in the contractile ring**

135 We first determined whether Pkd2 promotes the localization of Myo2 to the contractile ring. To
136 test this hypothesis, we compared the localization of the GFP tagged Myo2, expressed from its
137 endogenous locus, at the equatorial division plane of the hypomorphic *pkd2-81KD* mutant cells
138 (Morris et al., 2019) to that of the wild type cells using quantitative fluorescence microscopy
139 (Malla et al., 2022) (Fig. 1A). As in the wild type, GFP-Myo2 localized to a broad band of
140 cytokinesis nodes in the *pkd2* mutant cells before the nodes condensed into a complete
141 contractile ring (Fig. 1A and B). However, the contractile ring of the *pkd2* mutant cells matured
142 and constricted more quickly than that of the wild type cells (Fig. 1B), as reported previously
143 (Morris et al., 2019). GFP-Myo2 in the contractile ring of *pkd2* mutant cells increased by more
144 than 20% compared to the wild type cells (Fig. 1C and D). In contrast, the intracellular
145 concentration of GFP-Myo2, measured by its average fluorescence in a cell, was unchanged in
146 the mutant cells (Fig. 1E). Thus, Pkd2 modulates the assembly of Myo2 in the contractile ring
147 during cytokinesis.
148 Next, we considered whether Pkd2 helps recruit Rlc1, the regulatory light chain of Myo2
149 (Naqvi et al., 2000), to the contractile ring. This hypothesis is particularly attractive because Rlc1

150 possesses four EF-hands that bind the Pkd2-permeated Ca^{2+}. As we did above, we compared the
151 fluorescence of Rlc1 tagged endogenously with the fluorescence protein tdTomato (Rlc1-
152 tdTomato) in the contractile ring of *pkd2-81KD* cells to that of the wild type cells (Fig. 2A).
153 Similar to Myo2, the number of Rlc1-tdTomato molecules in the ring of the *pkd2* mutant cells
154 was ~20% higher than that of the wild type (Fig. 2B). Surprisingly, there was also a significant
155 increase (26%) of the intracellular concentration of Rlc1-tdTomato in the *pkd2* mutant cells,
156 compared to the wild type (Fig. 2E). Therefore, Pkd2 also modulates the recruitment of Rlc1 to
157 the contractile ring during cytokinesis.

158 Lastly, we determined whether Pkd2 has a role in the assembly of actin filaments in the
159 cytokinetic contractile ring. We employed GFP-Lifeact as the fluorescence reporter (Malla et al.,
160 2022) to quantify the number of actin molecules in the ring of *pkd2-81KD* and the wild type cells
161 (Fig. 3A). Overall, the actin patches of mutant cells were far more numerous than those of the
162 wild type cells and these patches distributed in a less polarized fashion (Fig. 3A). Nevertheless,
163 the assembly and disassembly of actin filaments in the contractile ring of the mutant cells
164 proceeded normally (Fig. 3B). In fact, the number of actin molecules in the contractile ring of
165 *pkd2-81KD* cells increased by 12% from that of the wild type cells (Fig. 3C). Interestingly, the
166 intracellular concentration of GFP-Lifeact in the mutant cells increased dramatically by almost
167 90% (Fig. 3D). Again, we concluded that Pkd2 modulates the assembly of actin filaments in the
168 cytokinetic contractile ring.

169 ***pkd2* and *myo2* play complementary roles in cytokinesis**

170 In an alternative approach, we examined the relationship between *pkd2* and *myo2,* both of which
171 are essential for cytokinesis through genetic studies. First, we confirmed the previously
172 discovered negative genetic interaction between *pkd2-81KD* and a temperature-sensitive mutant

173 *myo2-E1* (Morris et al., 2019). This finding is consistent with the negative genetic interaction
174 between the temperature-sensitive mutant *pkd2-B42* (Sinha et al., 2022) and *myo2-E1* (Fig. 4A).
175 As a result of this genetic interaction, the double mutant *pkd2-B42 myo2-E1* grew much more
176 slowly than either *pkd2-B42* or *myo2-E1* (Fig. 4A). Next, we compared the morphogenesis of
177 *pkd2-81KD, myo2-E1*, and *pkd2-81KD myo2-E1* cells. Morphologically, the double *pkd2 myo2*
178 mutant cells were similar to the *pkd2-81KD* cells. Both were rounder than the wild type.
179 However, the *pkd2 myo2* double mutant stood out for its large number of lysed cells (11±1.7%)
180 even at the permissive temperature of 25°C, far more than either the *pkd2* (5±0.5%) or *myo2*
181 (0.6±0.8%) mutant cells (Fig. 4B). The septation index of the double mutant (74%) was also
182 much higher than those of either single mutant (Fig. 4C). The septum of *pkd2-81KD myo2-E1*
183 cells were abnormal in their appearance. They were often wavy, a rare phenotype among either
184 of the single mutants. Lastly, a much higher fraction of the double mutant cells was multi-
185 septated (21±3%, averaged ± standard deviation, n>500) than either *pkd2-81KD* (10±1%) or
186 *myo2-E1* (1±0.1%). Based on these genetic analyses of the double *pkd2 myo2* mutant, we
187 concluded that *pkd2* and *myo2* play complementary roles in cytokinesis.

188 **Pkd2 synergizes with Myo2 to regulate the assembly of the contractile ring**

189 To determine how Pkd2 and Myo2 work synergistically in cytokinesis, we measured the
190 contractile ring assembly and constriction of the *pkd2-81KD myo2-E1* cells at the permissive
191 temperature through live fluorescence microscopy (Fig. 5A). These double mutant cells
192 assembled their contractile ring, marked by Rlc1-tdTomato, much more slowly than either *pkd2-*
193 *81KD* or *myo2-E1* cells (Fig. 5B). Strikingly, the contractile rings of most double mutant cells
194 (n=26) never appeared to be fully assembled. There were often many gaps in these contractile
195 rings (Fig. 5B). These rings nevertheless constricted at a rate comparable to those of either wild

196 type or *myo2-E1* cells at 25°C, but much more slowly than *pkd2-81KD* cells (Fig. 5C). We
197 concluded that both Pkd2 and Myo2 regulate the contractile ring assembly likely through
198 complementary pathways.

199 Lastly, we determined whether Pkd2 and Myo2 synergistically recruit the regulatory light
200 chain Rlc1 to the contractile ring. We measured the number of Rlc1-tdTomato molecules in the
201 contractile ring of the *pkd2-81KD myo2-E1* mutant cells through quantitative fluorescence
202 microscopy. Although Rlc1-Tdtomato continued to localize to the contractile ring of the *pkd2*
203 *myo2* double mutant cells (Fig. 5D), its number decreased dramatically (-60%) from that of the
204 *myo2-E1* cells (Fig. 5E). The intracellular concentration of Rlc1-tdTomato in the *pkd2 myo2*
205 double mutant cells decreased by a similar extent (-70%) (Fig. 5F). We concluded that both
206 Myo2 and Pkd2, likely through two complementary pathways, regulate the assembly of Rlc1 in
207 the contractile ring.

208 **Discussion**

209 In this study, we investigated whether the mechanosensitive calcium channel Pkd2 plays a role in
210 the assembly and constriction of the actomyosin contractile ring during cytokinesis. Through
211 quantitative fluorescence microscopy, we found surprisingly that Pkd2 mostly modulates the
212 assembly of the essential type II myosin Myo2, its regulatory light chain Rlc1 and actin filaments
213 in the contractile ring. Through analysis of the negative genetic interactions between *pkd2* and
214 *myo2* mutants, we found that Pkd2 and the type II myosin Myo2 work synergistically to promote
215 the assembly of the cytokinetic contractile ring.

216 The modulating role of Pkd2 in the contractile ring assembly is consistent with the
217 cytokinesis defects of the *pkd2-81KD* mutant cells. Our earlier works has found that the cleavage
218 furrow ingressed almost 50% more quickly in the *pkd2* mutant cells compared to the wild type
219 (Morris et al., 2019). This phenotype is in line with our new finding that the contractile ring of

220 the mutant cells contains 20% more Myo2, Rlc1 and actin than the wild type ones. The increased
221 densities of Myosin II and actin filaments shall in theory enhance the mechanical force generated
222 by the contractile ring. Combining this increased compressing force by the contractile ring of the
223 *pkd2* mutant with the reduced resistance from the outward turgor pressure (Sinha et al., 2022), it
224 is not surprising that the cleavage furrow ingresses so quickly in *pkd2-81KD* mutant cells.

225 The modulating effect of Pkd2 in the assembly of contractile ring most likely is rooted its
226 activity as a Ca^{2+}-permeable ion channel. In animal cells, Ca^{2+}-dependent myosin light chain
227 kinase (MLCK) phosphorylate Rlc in order to trigger the contractile ring constriction (Craig et
228 al., 1983). However, fission yeast does not possess a MLCK. Instead, its regulatory light chain
229 Rlc1 is phosphorylated by the kinase Pak1 during cytokinesis (Loo and Balasubramanian, 2008).
230 Although such phosphorylation of Rlc1 is not essential the temporal regulation of cytokinesis
231 (McCollum et al., 1999), it does promotes the assembly of actin filaments in the contractile ring
232 under stress condition (Prieto-Ruiz et al., 2023). Although Pak1 is not known as a
233 Ca^{2+}/calmodulin-dependent kinase, the contractile ring-localized phosphotase calcineurin is
234 (Martin-Garcia et al., 2018). We propose that calcineurin, a potential downstream target of Pkd2
235 channel, could dephosphorylate Rlc1 to modulate the assembly of the contractile ring.

236 It is surprising that mutations of *pkd2* significantly increase the intracellular
237 concentration of Rlc1 and actin. This could be due to the regulation of transcription by Pkd2. The
238 human polycystin PC1 does regulate gene transcription through its cleaved C-terminal
239 cytoplasmic tail (Chauvet et al., 2004). However, we have not observed nuclear localization of
240 Pkd2 so far. The alternative explanation could lie in the channel activity of Pkd2. Mutation of
241 this calcium permissive ion channel changes intracellular Ca^{2+} homeostasis (Poddar et al., 2022).
242 Ca^{2+}-sensitive phosphotase calcineurin. Calcineurin promotes the nuclear translocation and

243 activation of the transcription activator Prz1 (Hirayama et al., 2003). Therefore, Pkd2 may also
244 regulate the global gene transcription indirectly through the activation of calcineurin.

245 Considering the modulating effects of Pkd2 in the assembly of Myo2 at the contractile
246 ring, the negative genetic interaction between the *pkd2* and *myo2* mutants is surprising. Even
247 more surprising is our discovery that the abundance of Rlc1 in the contractile ring decreased
248 dramatically in the contractile ring of the *myo2 pkd2* double mutant cells. This is despite the fact
249 that *pkd2-81KD* mutation increases the number of Rlc1 in the contractile ring. A likely
250 explanation is that both Pkd2 and Myo2 promote the stability of the contractile ring. The Pkd2
251 channel may stabilize the contractile ring through modulating the assembly of actin and Myo2.
252 In contrast, Myo2 promotes the contractile ring stability through its motor activity, which is
253 comprised in the *myo2-E1* mutant (Balasubramanian et al., 1998). Our discovery suggests that
254 Pkd2 and Myo2 may play complementary roles in stabilizing the contractile ring during
255 cytokinesis.

256 Overall, our study demonstrated that the force-sensitive calcium channel Pkd2, although
257 not essential for the assembly of the contractile ring, plays a regulatory role in the assembly of
258 contractile ring through modulating the recruitment of actomyosin filaments to the ring. Future
259 work would determine whether Pkd2 exerts its regulatory function through its calcium
260 permeability and through it activation of the calcium-binding proteins such calmodulin and
261 calcineurin in cytokinesis.

262

263 **Author contributions**

264 Conceptualization, QC.; Methodology, QC, PC and DS; Software, QC; Validation, QC, PC, DS,
265 AP and MD; Formal Analysis, QC and PC; Investigation, QC, PC, DS, AP and MD; Resources,

266 QC, PC and DS; Data Curation, QC, PC and DS; Writing – Original Draft Preparation, QC and
267 PC; Writing – Review & Editing, QC and PC; Visualization, QC and PC; Supervision, QC;
268 Project Administration, QC; Funding Acquisition, QC.

269 **Competing interests**

270 The authors declare no competing interests.

271 **Acknowledgements**

272 We would like to thank the Chen lab members at The University of Toledo for technical
273 assistance. This work has been supported by the National Institutes of Health grant
274 R01GM144652 to QC and the National Science Foundation grant 2144701 to QC. The content is
275 solely the responsibility of the authors and does not necessarily represent the official views of the
276 National Institutes of Health. The authors declare no conflicts of interests.

277 **Table 1. List of yeast strains used in this study**.

Name	Genotype	Source
FY527	*h- leu1-32 ura4-D18 his3-D1 ade6-M216*	Lab stock
JW766	*h+ kanMX6-Pmyo2-GFP-myo2 ade6-M210 leu1-32 ura4-D18*	Wu Lab
JW1341	*h- rlc1-tdTomato-natMX6 ade6-M210 leu1-32 ura4-D18*	Wu Lab
QC-Y601	*h+ leu2::kanMX-Pcof1-mEGFP-Lifeact rlc1-tdTomato-Nat*	Lab stock
QC-Y799	*h+* myo2-E1 rlc1-tdTomato-NatMX6 sad1-mGFP-KanMX6	This study
QC-Y813	*h- kanMX6-81xnmt1-pkd2 rlc1-tdTomato-NatMX6*	Lab stock
QC-Y817	*h+ kanMX6-81xnmt1-pkd2 leu1-32 ura4-D18 his3-D1 ade6-M210*	Lab stock
QC-Y839	*h- myo2-E1*	
QC-Y840	*h+ myo2-E1 kanMX6-81xnmt1-Pkd2*	This study
QC-Y1033	*h? myo2-E1 kanMX6-81xnmt1-pkd2 rlc1-tdTomato-natMX6*	This study
QC-Y1112	*h? kanMX6-Pmyo2-GFP-myo2 ade6-M210 leu1-32 ura4-D18 kanMX6-81xnmt1-pkd2*	This study
QC-Y1156	*h? leu2::kanMX-Pcof1-mEGFP-Lifeact rlc1-tdTomato-Nat KanMX6-P81nmt1-pkd2 leu1-32 ura4-D18 his3-D1*	Lab stock
QC-Y1752	*h? pkd2::pkd2-B42-ura4+-hist5+ leu1-32 myo2-E1*	This study

278

Figure and Figure Legends

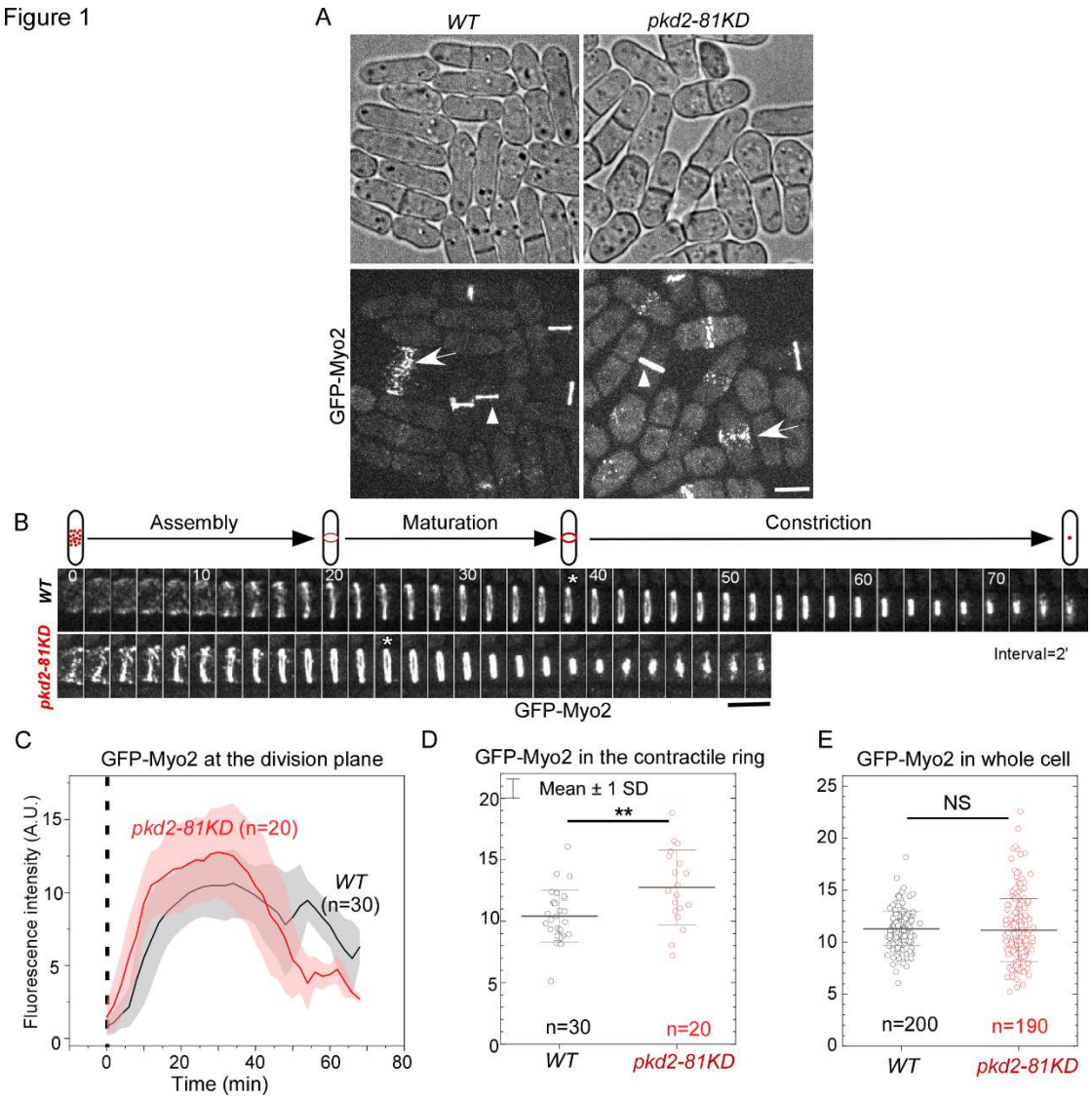

Figure 1: Localization of Myo2 in the contractile ring increased in *pkd2-81KD* cells. (A) Micrographs of wild type and *pkd2-81KD* cells expressing GFP-Myo2. Arrow: broad band of nodes. Arrowhead: the contractile ring. **(B)** Time lapse series of the equatorial plane of a wild type and a *pkd2-81KD* cells expressing GFP-Myo2. Top: a diagram of the contractile ring assembly, maturation and constriction in fission yeast cells. Asterisk: the start of contractile ring constriction. Number indicates time in minutes. Scale bar=5µm. **(C)** Time course of the fluorescence intensity of GFP-Myo2 at the equatorial plane after the start of contractile ring assembly (time zero). Cloud: standard deviations. **(D-E)** The dot plots of the average fluorescence intensity of GFP-Myo2 in either the contractile ring (D) or the whole cell (E). *: P<0.05. **: P<0.01. ***: P<0.001. N.S.: not significant. Statistics were calculated using two-tailed Student's t tests. All the data are pooled from at least two independent biological repeats. Scale bar=5µm.

Figure 2

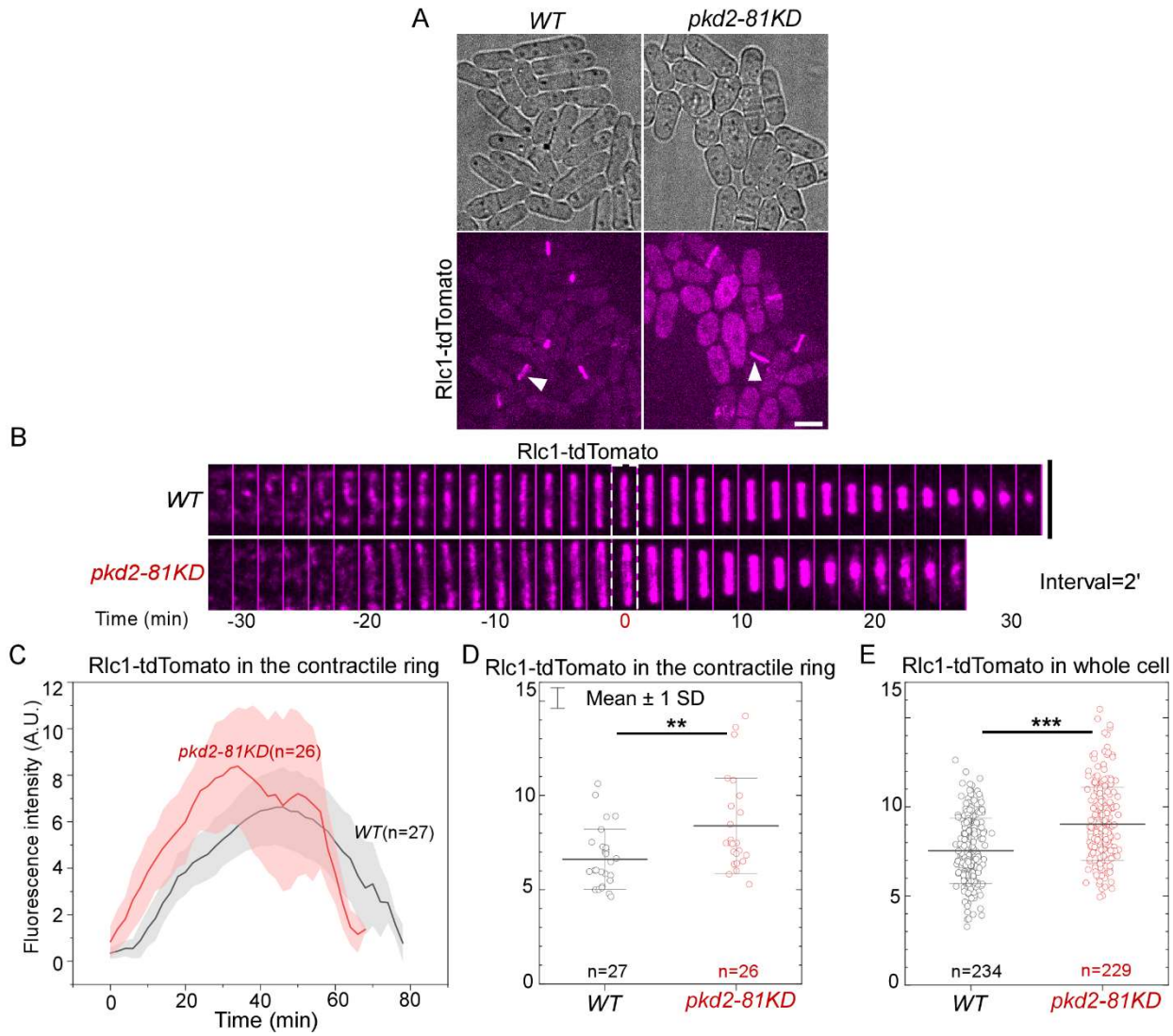

Figure 2: Localization of myosin light chain Rlc1 increased in *pkd2-81KD* mutant cells. (A) Micrographs of *wild type* and *pkd2-81KD* expressing Rlc1-tdTomato. Arrowhead: the contractile ring. **(B)** Time-lapse series of the equatorial plane of a *wild type* and a *pkd2-81KD* cell expressing Rlc1-tdTomato. Dashed box: the start of contractile ring constriction. Number indicates time in minutes. Scale bar=5µm. **(C)** Time course of the fluorescence intensity of Rlc1-tdTomato in the equatorial plane. Cloud: standard deviations. **(D-E)** Dot plots of the average fluorescence intensity of Rlc1-tdTomato in the mature contractile ring (D) or the whole cell (E). *: P<0.05. **: P<0.01. ***: P<0.001. N.S.: not significant. Statistics were calculated using two-tailed Student's t tests. All the data are pooled from at least two independent biological repeats.

Figure 3

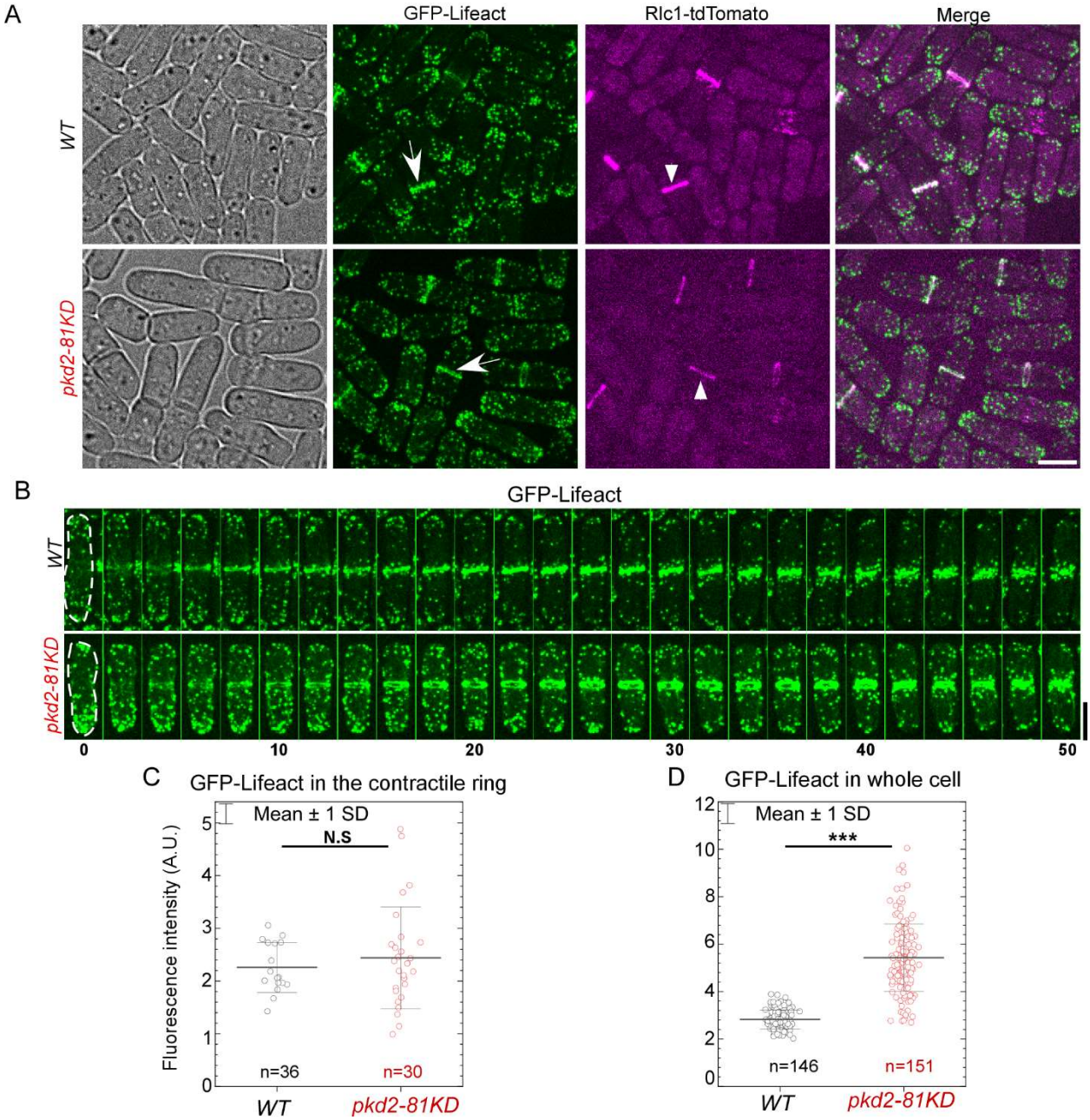

Figure 3: The number of actin molecules decreased in the contractile ring of *pkd2-B42* mutant cells. (A) Micrographs of the *wild type* and *pkd2-81KD* co-expressing GFP-Lifeact (green) and Rlc1-tdTomato (magenta). Arrow: GFP-Lifeact in division plane.Arrow-head: Rlc1-tdTomato in contractile ring. **(B)** Time series micrographs of a *wild type* and a *pkd2-81KD* cell. Number: time in minutes. Interval=2 mins. Scale bar=5µm. **(C-D)** Dot plots of the average fluorescence intensity of GFP-Lifeact in either the contractile ring (C) or the whole cell (D). *: P<0.05. **: P<0.01. ***: P<0.001. N.S.: not significant. Statistics were calculated using two-tailed Student's t tests. All the data are pooled from at least two independent biological repeats.

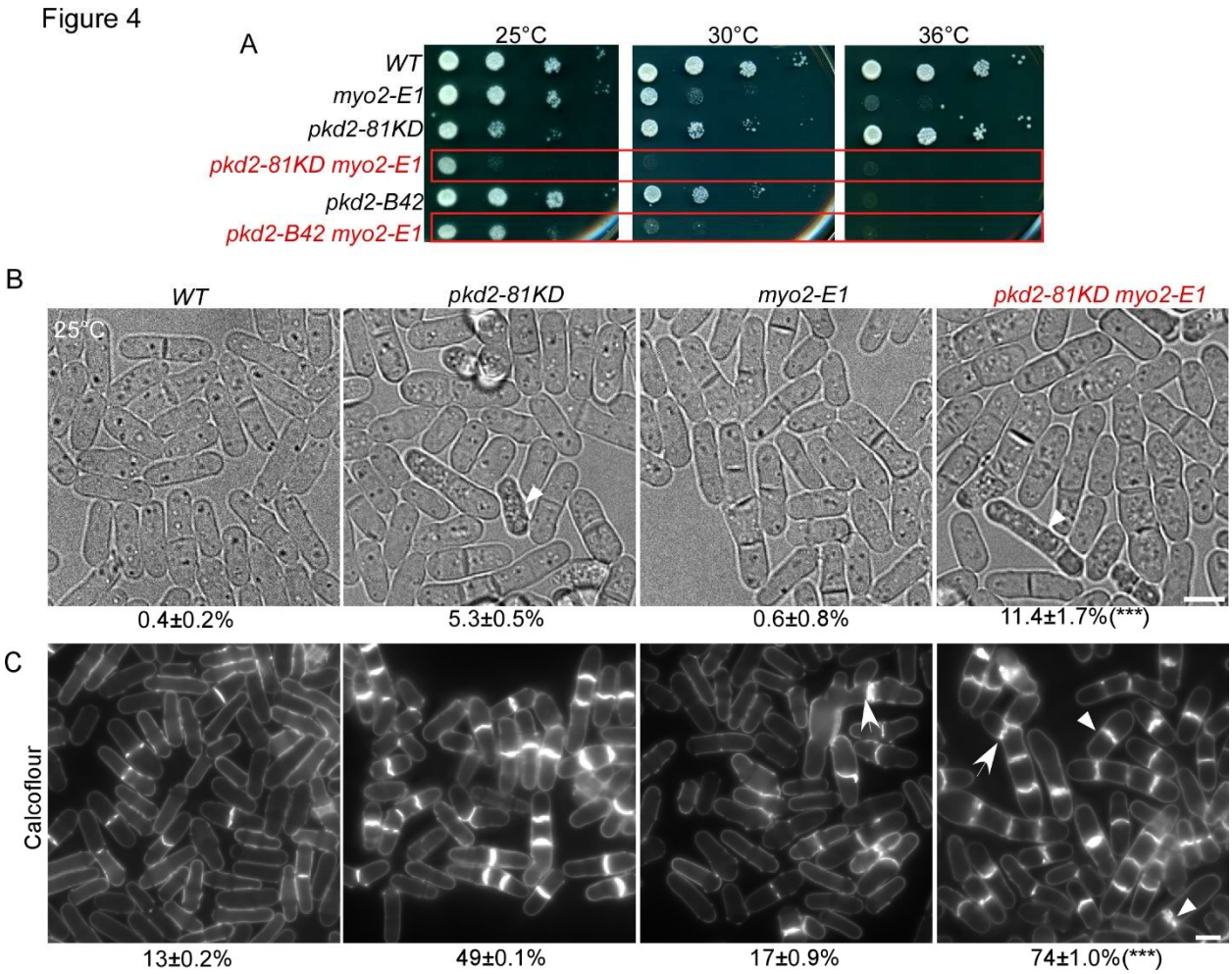

Figure 4: Genetic interactions among *pkd2* and *myo2* mutants. (A) Ten-fold dilution series of yeast cells at the indicated temperature after two days. **(B)** Bright-field micrographs of *pkd2-81KD, myo2-E1, and pkd2-81KD myo2-E1* cells at 25°C. Arrow: lysed cells. Number: average percentage of lysed cells ± standard deviations (n>200). **(C)** Micrographs of calcofluor stained cells at 25°C. Arrow: abnormal septum. Arrowhead: curved septum (n>500). All the data are pooled from at least two independent biological repeats. Scale bar=5µm.

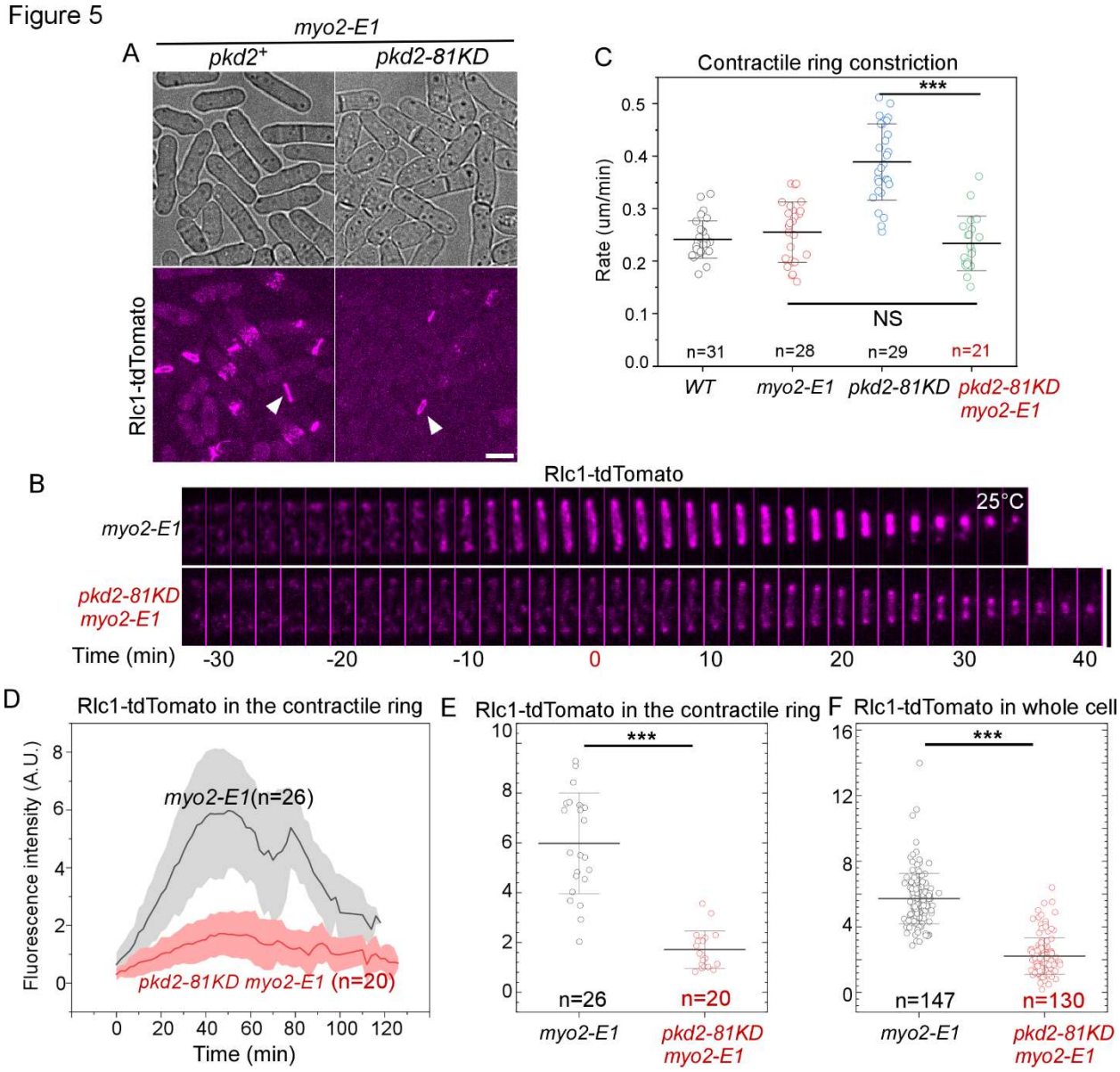

Figure 5: Localization of myosin regulatory light chain Rlc1 in the contractile ring decreased in the *pkd2-81KD myo2-E1* mutant cells. (A) Micrographs of *myo2-E1* and *pkd2-81KD myo2-E1* expressing Rlc1-tdTomato at 25°C. Arrow-heads: Rlc1-tdTomato in contractile ring. **(B)** Time-lapse series of the equatorial plane of a *myo2-E1* and a *pkd2-81KD myo2-E1* cell expressing Rlc1-tdTomato. Number indicates time in minutes. Scale bar=5µm. **(C)** Dot plots of the constriction rate of contractile ring at 25°C. **(D)** Time course of the fluorescence intensity of Rlc1-tdTomato at the equatorial plane. **(E-F)** Dot plots of average fluorescence intensity of Rlc1-tdTomato in either the contractile ring (E) or the whole cell (F). *: P<0.05. **: P<0.01. ***: P<0.001. N.S.: not significant. Statistics were calculated using two-tailed Student's t tests. All the data are pooled from at least two independent biological repeats.

334 **Reference**

335 Morris, Z., D. Sinha, A. Poddar, B. Morris, and Q. Chen. 2019. Fission yeast TRP channel Pkd2p
336 localizes to the cleavage furrow and regulates cell separation during cytokinesis.
337 *Molecular biology of the cell*. 30:1791-1804.

338 Courtemanche, N., T.D. Pollard, and Q. Chen. 2016. Avoiding artefacts when counting
339 polymerized actin in live cells with LifeAct fused to fluorescent proteins. *Nature cell*
340 *biology*. 18:676-683.
341 Malla, M., T.D. Pollard, and Q. Chen. 2022. Counting actin in contractile rings reveals novel
342 contributions of cofilin and type II myosins to fission yeast cytokinesis. *Molecular*
343 *biology of the cell*. 33:ar51.

344 1994. The polycystic kidney disease 1 gene encodes a 14 kb transcript and lies within a
345 duplicated region on chromosome 16. The European Polycystic Kidney Disease
346 Consortium. *Cell*. 77:881-894.
347 AbouAlaiwi, W.A., S. Ratnam, R.L. Booth, J.V. Shah, and S.M. Nauli. 2011. Endothelial cells
348 from humans and mice with polycystic kidney disease are characterized by polyploidy
349 and chromosome segregation defects through survivin down-regulation. *Human*
350 *molecular genetics*. 20:354-367.
351 Balasubramanian, M.K., D. McCollum, L. Chang, K.C. Wong, N.I. Naqvi, X. He, S. Sazer, and
352 K.L. Gould. 1998. Isolation and characterization of new fission yeast cytokinesis
353 mutants. *Genetics*. 149:1265-1275.
354 Chauvet, V., X. Tian, H. Husson, D.H. Grimm, T. Wang, T. Hiesberger, P. Igarashi, A.M.
355 Bennett, O. Ibraghimov-Beskrovnaya, S. Somlo, and M.J. Caplan. 2004. Mechanical
356 stimuli induce cleavage and nuclear translocation of the polycystin-1 C terminus. *The*
357 *Journal of clinical investigation*. 114:1433-1443.
358 Chen, Q., and T.D. Pollard. 2011. Actin filament severing by cofilin is more important for
359 assembly than constriction of the cytokinetic contractile ring. *The Journal of cell biology*.
360 195:485-498.
361 Craig, R., R. Smith, and J. Kendrick-Jones. 1983. Light-chain phosphorylation controls the
362 conformation of vertebrate non-muscle and smooth muscle myosin molecules. *Nature*.
363 302:436-439.
364 Hardy, E., and L. Tsiokas. 2020. Polycystins as components of large multiprotein complexes of
365 polycystin interactors. *Cellular signalling*. 72:109640.
366 Hirayama, S., R. Sugiura, Y. Lu, T. Maeda, K. Kawagishi, M. Yokoyama, H. Tohda, Y. Giga-
367 Hama, H. Shuntoh, and T. Kuno. 2003. Zinc finger protein Prz1 regulates Ca2+ but not
368 Cl- homeostasis in fission yeast. Identification of distinct branches of calcineurin
369 signaling pathway in fission yeast. *The Journal of biological chemistry*. 278:18078-
370 18084.
371 Hu, J., and P.C. Harris. 2020. Regulation of polycystin expression, maturation and trafficking.
372 *Cellular signalling*. 72:109630.
373 Kovar, D.R., V. Sirotkin, and M. Lord. 2011. Three's company: the fission yeast actin
374 cytoskeleton. *Trends in cell biology*. 21:177-187.
375 Laplante, C., J. Berro, E. Karatekin, A. Hernandez-Leyva, R. Lee, and T.D. Pollard. 2015. Three
376 myosins contribute uniquely to the assembly and constriction of the fission yeast
377 cytokinetic contractile ring. *Curr Biol*. 25:1955-1965.

378 Loo, T.H., and M. Balasubramanian. 2008. Schizosaccharomyces pombe Pak-related protein,
379 Pak1p/Orb2p, phosphorylates myosin regulatory light chain to inhibit cytokinesis. *The*
380 *Journal of cell biology*. 183:785-793.
381 Malla, M., T.D. Pollard, and Q. Chen. 2022. Counting actin in contractile rings reveals novel
382 contributions of cofilin and type II myosins to fission yeast cytokinesis. *Molecular*
383 *biology of the cell*. 33:ar51.
384 Malla, M., D. Sinha, P. Chowdhury, B.T. Bisesi, and Q. Chen. 2023. The cytoplasmic tail of the
385 mechanosensitive channel Pkd2 regulates its internalization and clustering in eisosomes.
386 *Journal of cell science*. 136.
387 Martin-Garcia, R., V. Arribas, P.M. Coll, M. Pinar, R.A. Viana, S.A. Rincon, J. Correa-Bordes,
388 J.C. Ribas, and P. Perez. 2018. Paxillin-Mediated Recruitment of Calcineurin to the
389 Contractile Ring Is Required for the Correct Progression of Cytokinesis in Fission Yeast.
390 *Cell reports*. 25:772-783 e774.
391 McCollum, D., A. Feoktistova, and K.L. Gould. 1999. Phosphorylation of the myosin-II light
392 chain does not regulate the timing of cytokinesis in fission yeast. *The Journal of*
393 *biological chemistry*. 274:17691-17695.
394 Mochizuki, T., G. Wu, T. Hayashi, S.L. Xenophontos, B. Veldhuisen, J.J. Saris, D.M. Reynolds,
395 Y. Cai, P.A. Gabow, A. Pierides, W.J. Kimberling, M.H. Breuning, C.C. Deltas, D.J.
396 Peters, and S. Somlo. 1996. PKD2, a gene for polycystic kidney disease that encodes an
397 integral membrane protein. *Science (New York, N.Y)*. 272:1339-1342.
398 Moreno, S., A. Klar, and P. Nurse. 1991. Molecular genetic analysis of fission yeast
399 Schizosaccharomyces pombe. *Methods in enzymology*. 194:795-823.
400 Morris, Z., D. Sinha, A. Poddar, B. Morris, and Q. Chen. 2019. Fission yeast TRP channel Pkd2p
401 localizes to the cleavage furrow and regulates cell separation during cytokinesis.
402 *Molecular biology of the cell*. 30:1791-1804.
403 Naqvi, N.I., K.C. Wong, X. Tang, and M.K. Balasubramanian. 2000. Type II myosin regulatory
404 light chain relieves auto-inhibition of myosin-heavy-chain function. *Nature cell biology*.
405 2:855-858.
406 Palmer, C.P., E. Aydar, and M.B. Djamgoz. 2005. A microbial TRP-like polycystic-kidney-
407 disease-related ion channel gene. *The Biochemical journal*. 387:211-219.
408 Poddar, A., Y.Y. Hsu, F. Zhang, A. Shamma, Z. Kreais, C. Muller, M. Malla, A. Ray, A. Liu,
409 and Q. Chen. 2022. Membrane stretching activates calcium-permeability of a putative
410 channel Pkd2 during fission yeast cytokinesis. *Molecular biology of the*
411 *cell*:mbcE22070248.
412 Poddar, A., O. Sidibe, A. Ray, and Q. Chen. 2021. Calcium spikes accompany cleavage furrow
413 ingression and cell separation during fission yeast cytokinesis. *Molecular biology of the*
414 *cell*. 32:15-27.
415 Pollard, T.D., and J.Q. Wu. 2010. Understanding cytokinesis: lessons from fission yeast. *Nature*
416 *reviews*. 11:149-155.
417 Prieto-Ruiz, F., E. Gomez-Gil, R. Martin-Garcia, A.J. Perez-Diaz, J. Vicente-Soler, A. Franco,
418 T. Soto, P. Perez, M. Madrid, and J. Cansado. 2023. Myosin II regulatory light chain
419 phosphorylation and formin availability modulate cytokinesis upon changes in
420 carbohydrate metabolism. *eLife*. 12.
421 Shen, P.S., X. Yang, P.G. DeCaen, X. Liu, D. Bulkley, D.E. Clapham, and E. Cao. 2016. The
422 Structure of the Polycystic Kidney Disease Channel PKD2 in Lipid Nanodiscs. *Cell*.
423 167:763-773 e711.

424 Sinha, D., D. Ivan, E. Gibbs, M. Chetluru, J. Goss, and Q. Chen. 2022. Fission yeast polycystin
425 Pkd2p promotes cell size expansion and antagonizes the Hippo-related SIN pathway.
426 *Journal of cell science*. 135.
427 Su, Q., F. Hu, X. Ge, J. Lei, S. Yu, T. Wang, Q. Zhou, C. Mei, and Y. Shi. 2018. Structure of the
428 human PKD1-PKD2 complex. *Science (New York, N.Y)*. 361.
429 Ta, C.M., T.N. Vien, L.C.T. Ng, and P.G. DeCaen. 2020. Structure and function of polycystin
430 channels in primary cilia. *Cellular signalling*. 72:109626.
431 Thevenaz, P., U.E. Ruttimann, and M. Unser. 1998. A pyramid approach to subpixel registration
432 based on intensity. *IEEE Trans Image Process*. 7:27-41.
433 Wu, J.Q., and T.D. Pollard. 2005. Counting cytokinesis proteins globally and locally in fission
434 yeast. *Science (New York, N.Y)*. 310:310-314.

435

Figure 5

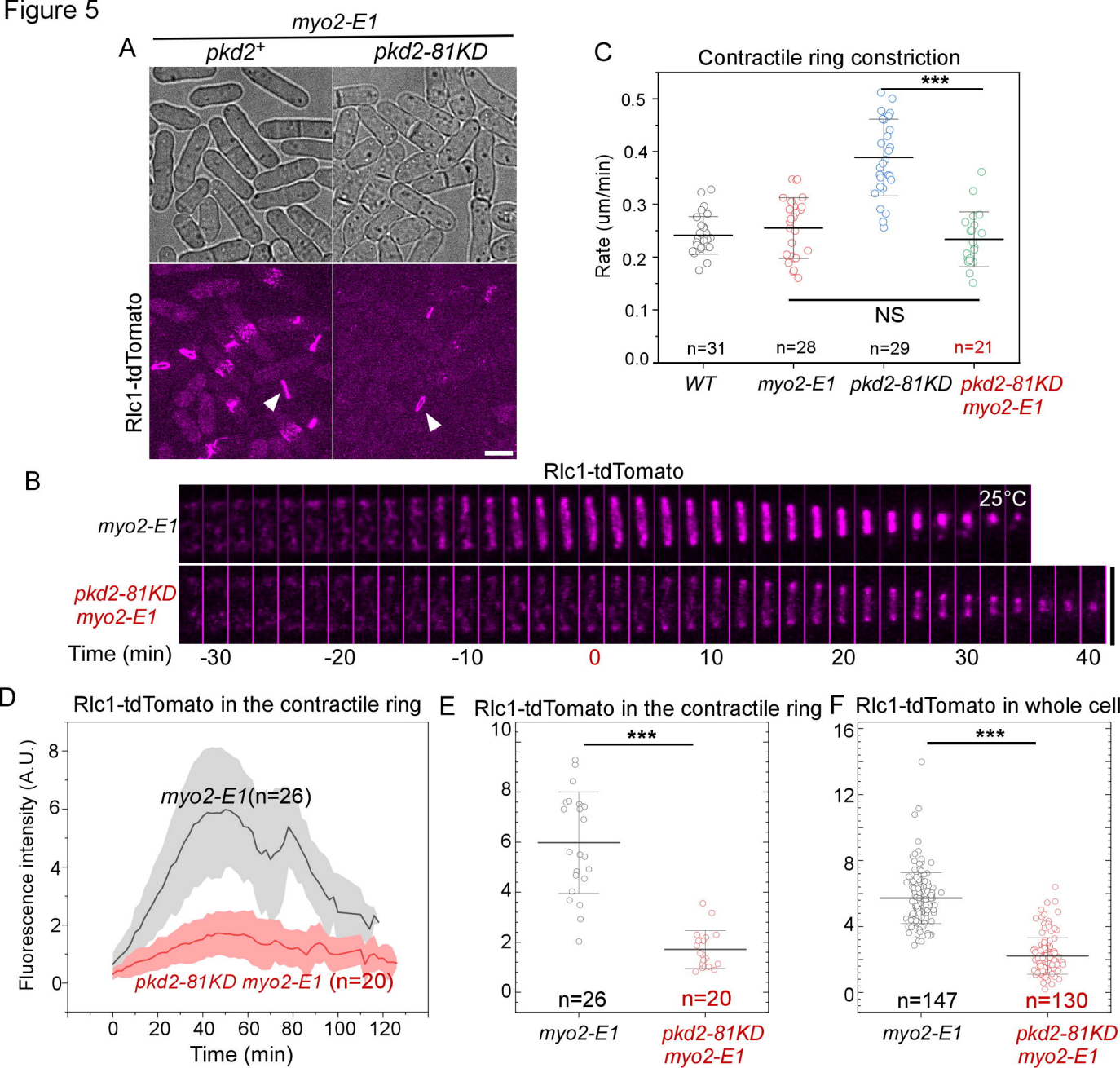
A
myo2-E1
pkd2+
pkd2-81KD
Rlc1-tdTomato
C
Contractile ring constriction
***
Rate (um/min)
0.0
0.1
0.2
0.3
0.4
0.5
NS
n=31
n=28
n=29
n=21
WT
myo2-E1
pkd2-81KD
pkd2-81KD myo2-E1
B
Rlc1-tdTomato
25°C
myo2-E1
pkd2-81KD myo2-E1
Time (min)
-30
-20
-10
0
10
20
30
40
D
Rlc1-tdTomato in the contractile ring
Fluorescence intensity (A.U.)
myo2-E1(n=26)
pkd2-81KD myo2-E1 (n=20)
Time (min)
0
20
40
60
80
100
120
E
Rlc1-tdTomato in the contractile ring
***
n=26
n=20
myo2-E1
pkd2-81KD myo2-E1
F
Rlc1-tdTomato in whole cell
***
n=147
n=130
myo2-E1
pkd2-81KD myo2-E1

Figure 4

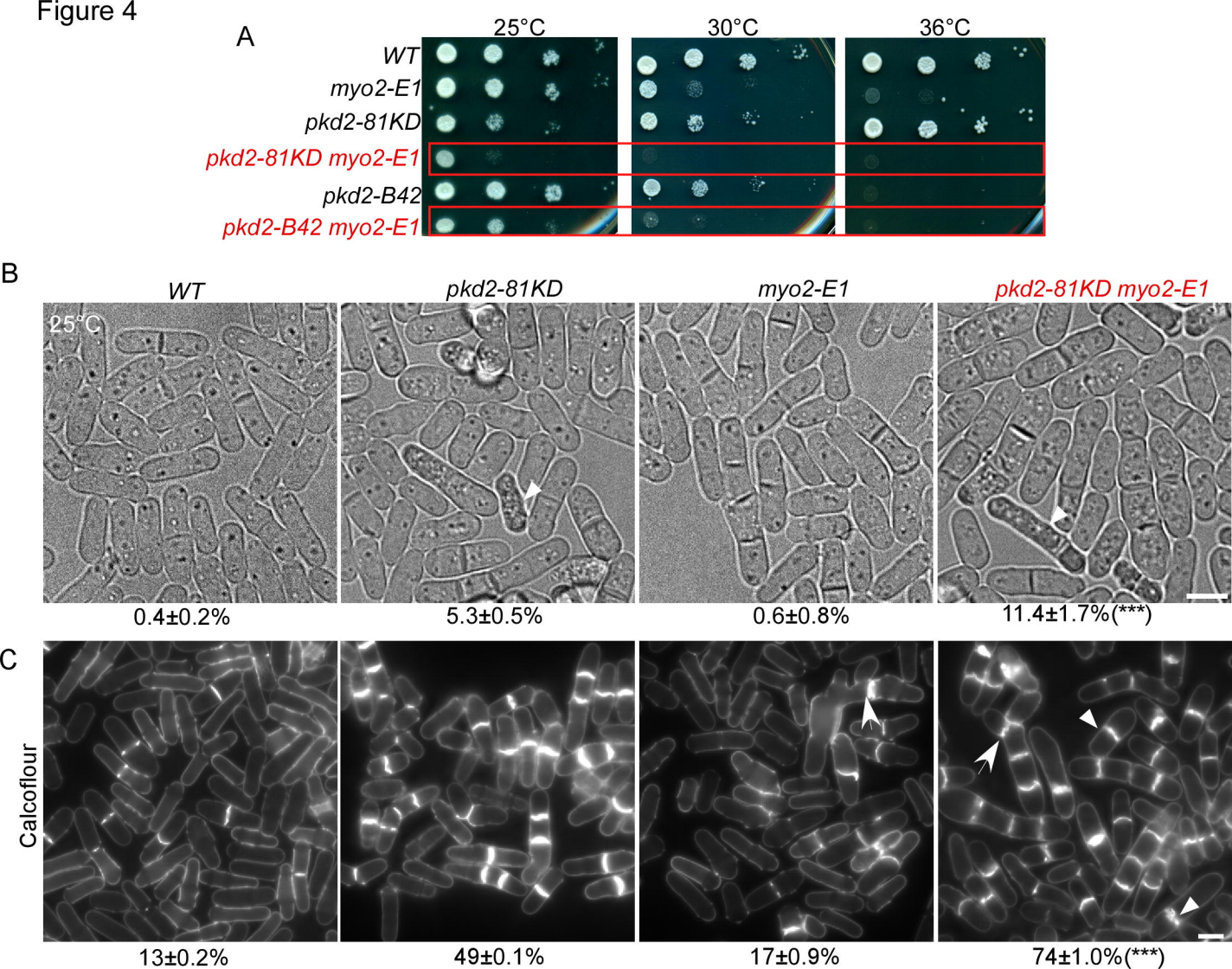
A
25°C
30°C
36°C
WT
myo2-E1
pkd2-81KD
pkd2-81KD myo2-E1
pkd2-B42
pkd2-B42 myo2-E1
B
WT
pkd2-81KD
myo2-E1
pkd2-81KD myo2-E1
25°C
0.4±0.2%
5.3±0.5%
0.6±0.8%
11.4±1.7%(***)
C
Calcoflour
13±0.2%
49±0.1%
17±0.9%
74±1.0%(***)

Figure 3

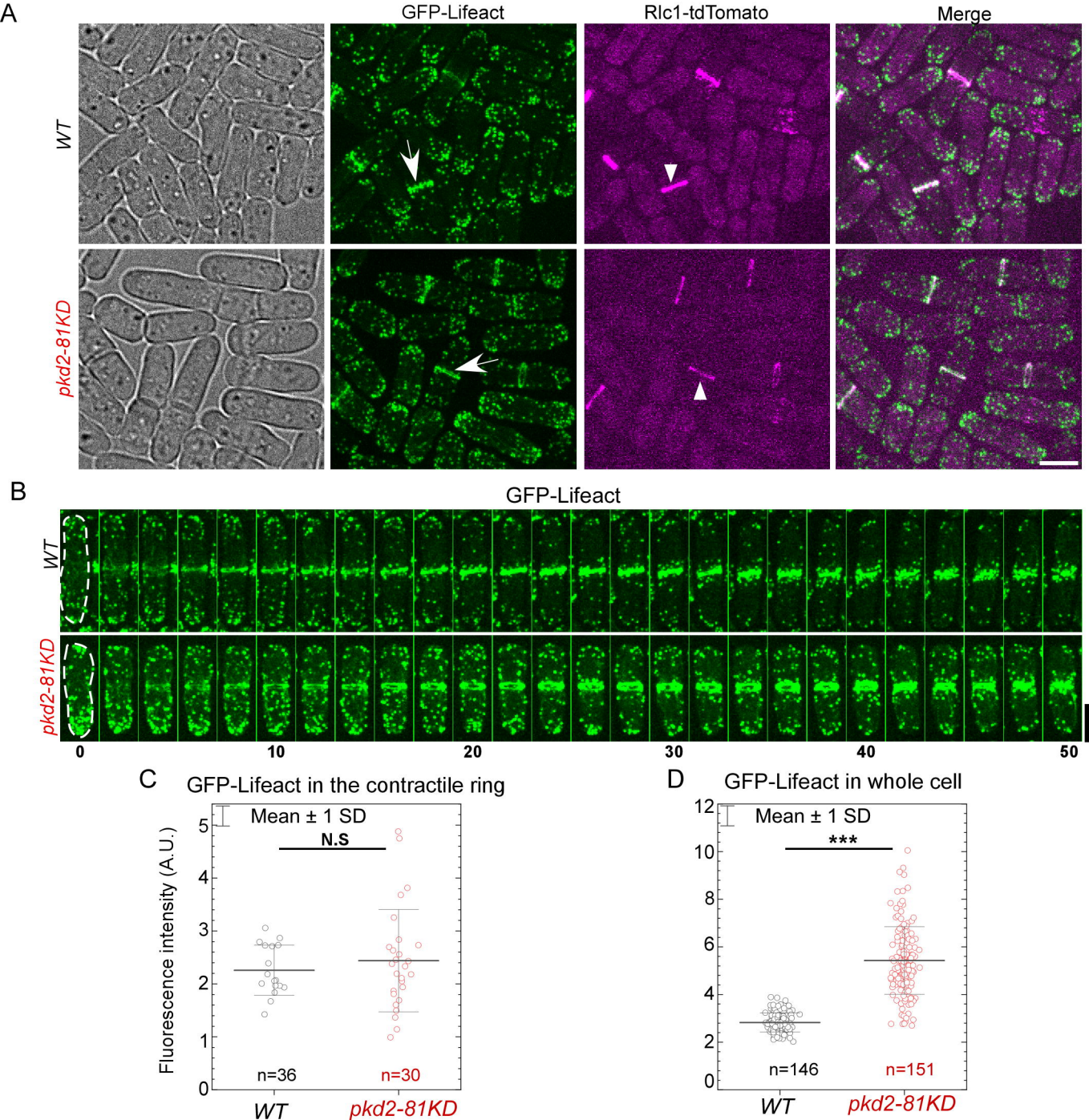
A
GFP-Lifeact
Rlc1-tdTomato
Merge
WT
pkd2-81KD
B
GFP-Lifeact
WT
pkd2-81KD
0
10
20
30
40
50
C
GFP-Lifeact in the contractile ring
Mean ± 1 SD
N.S
Fluorescence intensity (A.U.)
n=36
n=30
WT
pkd2-81KD
D
GFP-Lifeact in whole cell
Mean ± 1 SD
***
n=146
n=151
WT
pkd2-81KD

Figure 2

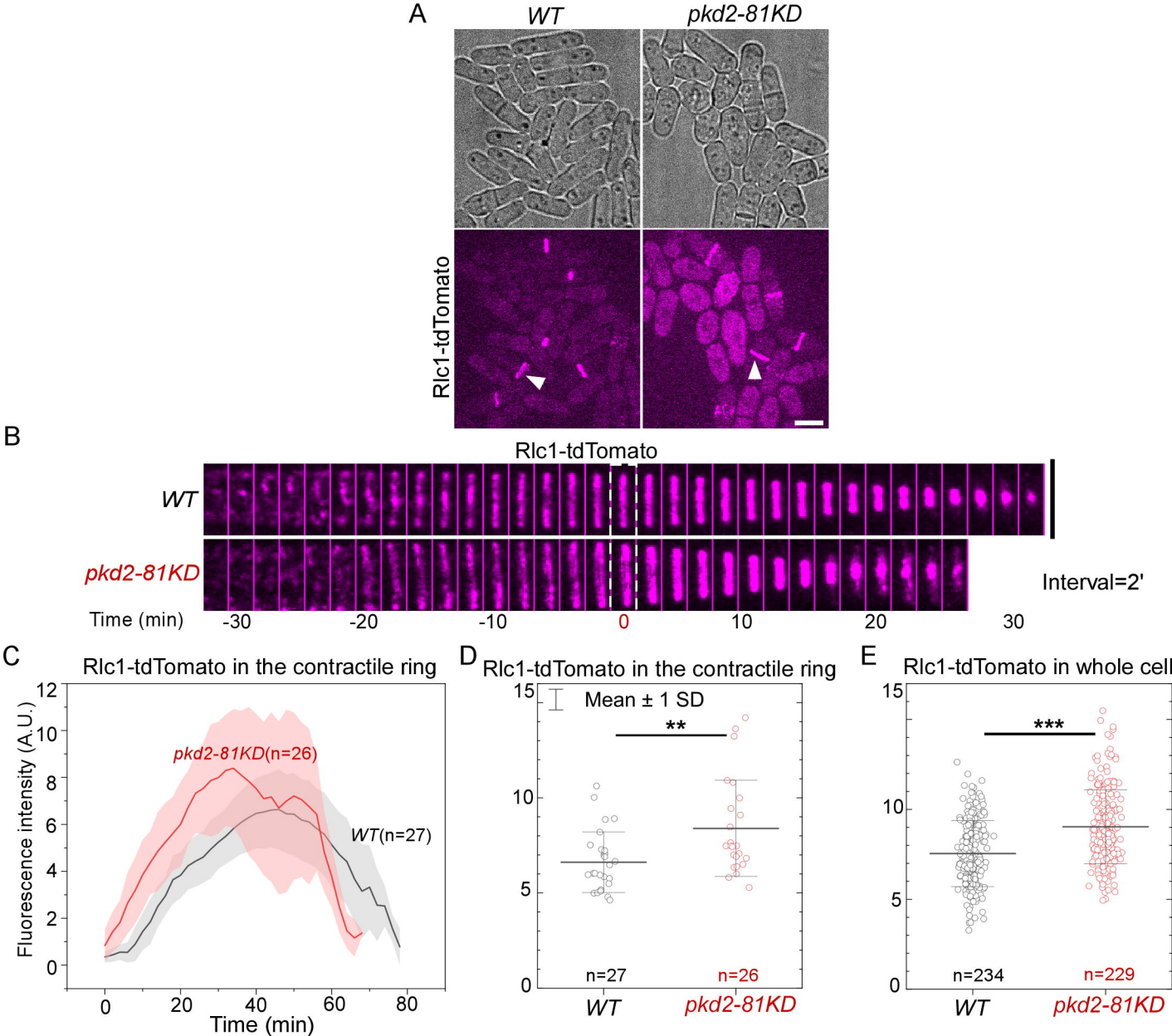
A
WT
pkd2-81KD
Rlc1-tdTomato
B
Rlc1-tdTomato
WT
pkd2-81KD
Interval=2'
Time (min)
-30
-20
-10
0
10
20
30
C
Rlc1-tdTomato in the contractile ring
Fluorescence intensity (A.U.)
pkd2-81KD(n=26)
WT(n=27)
Time (min)
D
Rlc1-tdTomato in the contractile ring
Mean ± 1 SD
**
n=27
n=26
WT
pkd2-81KD
E
Rlc1-tdTomato in whole cell
***
n=234
n=229
WT
pkd2-81KD

Figure 1

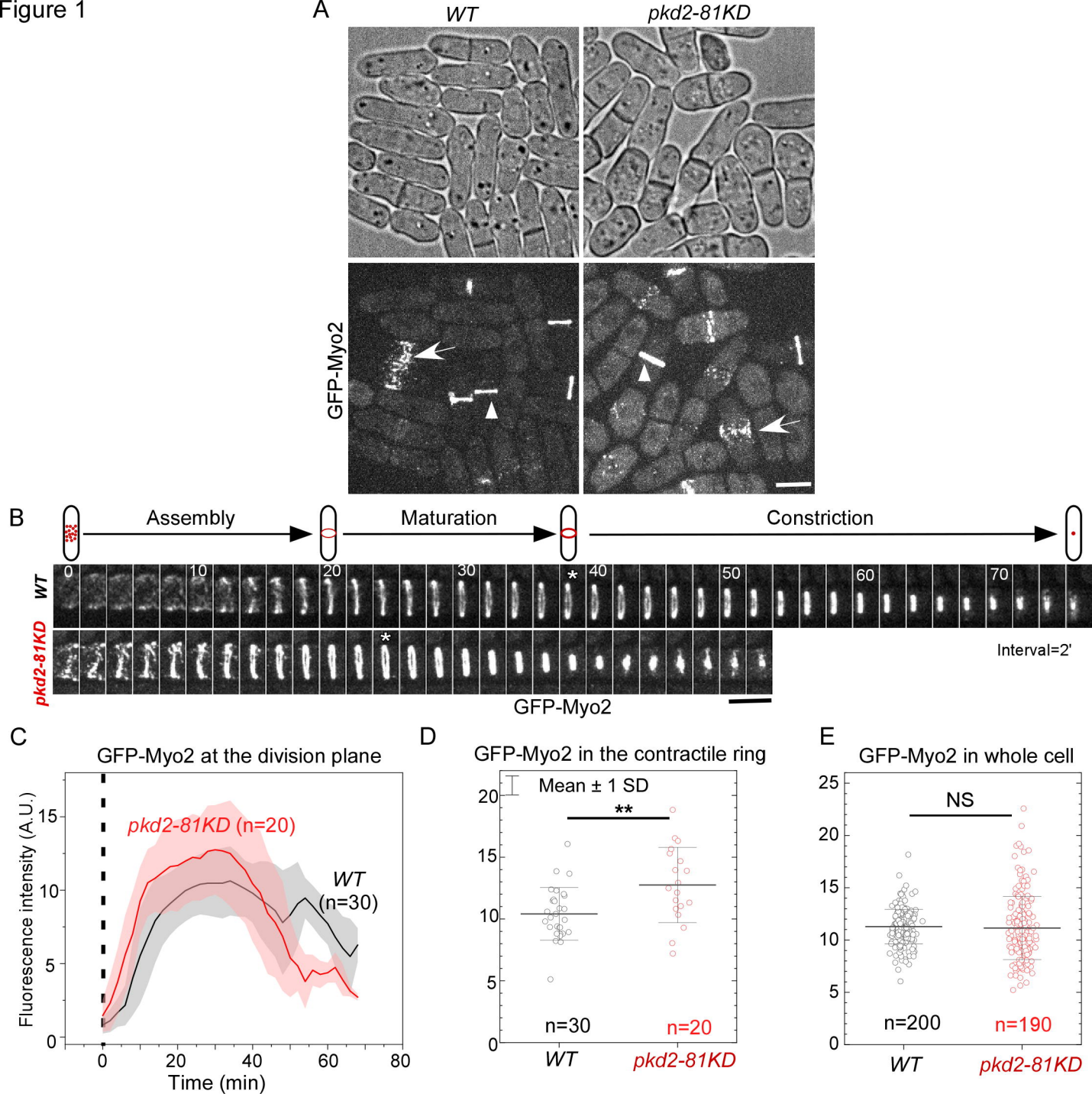
A
WT
pkd2-81KD
GFP-Myo2
B
Assembly
Maturation
Constriction
WT
pkd2-81KD
0
10
20
30
40
50
60
70
Interval=2'
GFP-Myo2
C
GFP-Myo2 at the division plane
pkd2-81KD (n=20)
WT
(n=30)
Fluorescence intensity (A.U.)
Time (min)
D
GFP-Myo2 in the contractile ring
Mean ± 1 SD
**
n=30
n=20
WT
pkd2-81KD
E
GFP-Myo2 in whole cell
NS
n=200
n=190
WT
pkd2-81KD